Available online at www.sciencedirect.com
SCIENCE DIRECT®
Journal of Organometallic Chemistry 670 (2003) 248–255
Journal of Organometallic Chemistry
www.elsevier.com/locate/jorganchem

Organometallic complexes for nonlinear optics Part 32: Synthesis, optical spectroscopy and theoretical studies of some osmium alkynyl complexes☆

Joseph P. Morrall [a], Clem E. Powell [a], Robert Stranger [a], Marie P. Cifuentes [a,*], Mark G. Humphrey [a], Graham A. Heath [b]

[a] Department of Chemistry, Australian National University, Canberra, ACT 0200, Australia
[b] Research School of Chemistry, Australian National University, Canberra, ACT 0200, Australia

Received 10 January 2003; received in revised form 10 January 2003; accepted 15 January 2003

Abstract

The complexes *trans*-[Os(C≡CPh)Cl(dppe)$_2$] (**1**), *trans*-[Os(4-C≡CC$_6$H$_4$C≡CPh)Cl(dppe)$_2$] (**2**), and 1,3,5-{*trans*-[OsCl(dppe)$_2$(4-C≡CC$_6$H$_4$C≡C)]}$_3$C$_6$H$_3$ (**3**) have been prepared. Cyclic voltammetric studies reveal a quasi-reversible oxidation process for each complex at 0.36–0.39 V (with respect to the ferrocene/ferrocenium couple at 0.56 V), assigned to the $Os^{II/III}$ couple. In situ oxidation of **1**–**3** using an optically transparent thin-layer electrochemical (OTTLE) cell affords the UV–Vis–NIR spectra of the corresponding cationic complexes **1**$^+$–**3**$^+$; a low-energy band is observed in the near-IR region (11 000–14 000 cm^{-1}) in each case, in contrast to the neutral complexes **1**–**3** which are optically transparent below 20 000 cm^{-1}. Density functional theory calculations on the model compounds *trans*-[Os(C≡CPh)Cl(PH$_3$)$_4$] and *trans*-[Os(4-C≡CC$_6$H$_4$C≡CPh)Cl(PH$_3$)$_4$] have been used to rationalize the observed optical spectra and suggest that the low-energy bands in the spectra of the cationic complexes can be assigned to transitions involving orbitals delocalized over the metal, chloro and alkynyl ligands. These intense bands have potential utility in switching nonlinear optical response, of interest in optical technology.

Keywords: Osmium; Acetylide; Spectroelectrochemistry; Optical spectroscopy; Density functional theory

1. Introduction

The optical properties of metal alkynyl complexes have been of recent interest for a number of reasons, including their possible application in nonlinear optical (NLO) technology [2–4]. Although organic compounds have dominated recent studies of molecular NLO materials, inorganic complexes may have a number of advantages, e.g., switchability of NLO properties by accessing different oxidation states of the metal center [5–9]. We have recently reported the UV–Vis–NIR spectroelectrochemical properties of the series of linear ruthenium alkynyl complexes *trans*-[RuXY(dppe)$_2$] [dppe = 1,2-bis(diphenylphosphino)ethane; X = Cl, Y = Cl, C≡CPh, 4-C≡CC$_6$H$_4$C≡CPh; X = C≡CPh, Y = C≡CPh, 4-C≡CC$_6$H$_4$C≡CPh] and of their corresponding cationic analogues obtained by in situ oxidation of the alkynyl complexes using an optically transparent thin-layer electrochemical (OTTLE) cell [6]. A comparison with similar spectral studies of the related octopolar complex 1,3,5-{*trans*-[RuCl(dppe)$_2$(4-C≡CC$_6$H$_4$C≡C)]}$_3$C$_6$H$_3$ [5] has demonstrated the emergence of low-energy absorptions in the electronic spectra of the oxidized species which progress to lower energy on moving from the mono-alkynyl complexes *trans*-[Ru(C≡CPh)Cl(dppe)$_2$] (12 040 cm^{-1}) and *trans*-[Ru(4-C≡CC$_6$H$_4$C≡CPh)Cl(dppe)$_2$] (11 160 cm^{-1}) to the bis-alkynyl complexes *trans*-[Ru(C≡CPh)$_2$(dppe)$_2$] (8920

☆ For Part 31, see Ref. [1].

* Corresponding author. Tel.: +61-2-6125-4293; fax: +61-2-6125-0760.
E-mail address: marie.cifuentes@anu.edu.au (M.P. Cifuentes).

0022-328X/03/$ - see front matter © 2003 Published by Elsevier Science B.V.
doi:10.1016/S0022-328X(03)00039-1

cm^{-1}) and *trans*-[Ru(C≡CPh)(4-C≡CC_6H_4C≡CPh)-$(dppe)_2$] (8440 cm^{-1}), with the octopolar triruthenium complex, 1,3,5-{*trans*-[RuCl$(dppe)_2$(4-C≡CC_6H_4C≡C)]}$_3C_6H_3$ (11 200 cm^{-1}), emulating the mono-alkynyl complexes as expected by the similarity of their coordination spheres. Time-dependent density functional theory (TD-DFT) applied to model linear ruthenium alkynyl complexes (replacing dppe by PH_3) show the dominant low-energy transitions in the electronic spectra of the neutral species to be predominantly metal-to-alkynyl charge transfer processes, and the low-energy transitions in the electronic spectra of the oxidized species to be largely chloro/alkynyl-to-metal charge transfer in character [6].

We have previously shown that the back-bonding interaction between the metal and alkynyl ligand, which may be important for maximizing NLO response, increases on proceeding from ruthenium to osmium [10], and so an examination of the corresponding osmium complexes is clearly of interest. Few suitable bis(bidentate phosphine)osmium alkynyl complexes are extant [11–20], and none thus far have been reported utilizing the ubiquitous diphosphine dppe. With this in mind, we report herein a synthetic, spectroelectrochemical and TD-DFT study of the series of osmium alkynyl complexes *trans*-[Os(C≡CPh)Cl$(dppe)_2$] (**1**), *trans*-[Os(4-C≡CC_6H_4C≡CPh)Cl$(dppe)_2$] (**2**), and 1,3,5-{*trans*-[OsCl$(dppe)_2$(4-C≡CC_6H_4C≡C)]}$_3C_6H_3$ (**3**), which provides the opportunity to assess the effect of chain-lengthening, progression from linear to branched geometry, and metal variation on the optical properties which are crucial for NLO responses.

2. Results and discussion

2.1. Synthesis and characterization of σ-acetylide complexes

The syntheses of the osmium alkynyl complexes *trans*-[Os(C≡CPh)Cl$(dppe)_2$] (**1**), *trans*-[Os(4-C≡CC_6H_4C≡CPh)Cl$(dppe)_2$] (**2**), and 1,3,5-{*trans*-[OsCl$(dppe)_2$(4-C≡CC_6H_4C≡C)]}$_3C_6H_3$ (**3**) (Scheme 1) were carried out by procedures similar to those successfully employed for the syntheses of the analogous ruthenium alkynyl complexes [6,21,22]. In each case, *cis*-[$OsCl_2(dppe)_2$] is allowed to react with the appropriate acetylene in refluxing toluene in the presence of ammonium hexafluorophosphate for 18 h, before addition of triethylamine, affording the alkynylosmium complexes in moderate yields. Varying the reaction times and temperature did not improve product yields.

The new osmium alkynyl complexes were characterized by chemical ionization and secondary ion mass spectrometry, UV–Vis and IR spectroscopy, and ^{1}H- and ^{31}P-NMR spectroscopy. It proved extremely difficult to obtain satisfactory analyses, a problem experienced previously in related osmium alkynyl complex synthesis [12]. The mass spectrum of **2** contains a molecular ion, with fragmentation proceeding by competitive loss of chloro and alkynyl ligands. In contrast, the mass spectrum of **3** contains a fragment ion at highest *m*/*z* value corresponding to one "arm" of the octopolar complex. All complexes contain ions in their mass spectra corresponding to $[OsCl(CO)(dppe)_2]^+$, likely to result from oxidation at the alkynyl group, or perhaps the protonated (vinylidene) complexes; oxida-

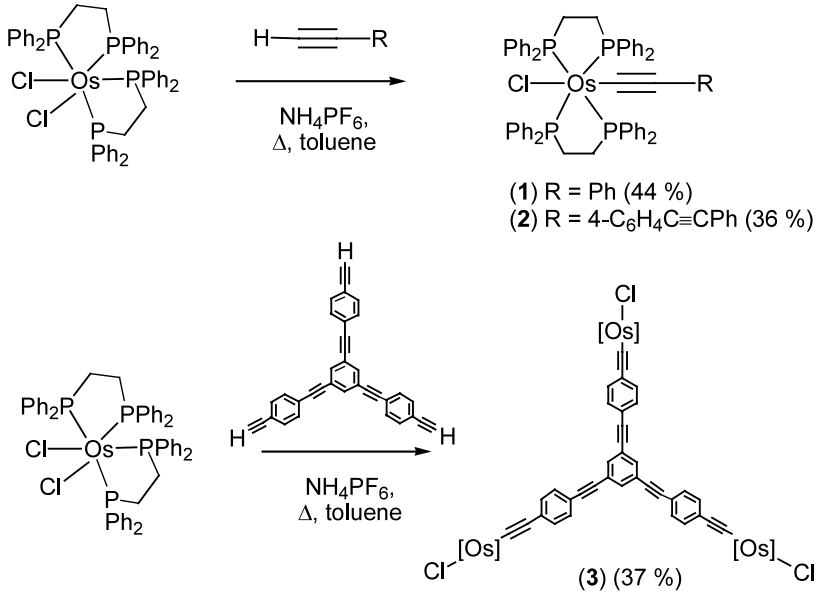

Scheme 1. Syntheses of alkynylosmium complexes **1**–**3**.

tion of ruthenium vinylidene complexes is known to afford the corresponding carbonyl cationic complexes. The IR spectra for **1–3** contain ν(C≡C) bands at similar frequencies (2057–2065 cm^{-1}), as expected. The UV–Vis spectra contain lowest energy bands in the range 31 000–22 000 cm^{-1}, which may be assigned to the MLCT transition from the metal-to-alkynyl ligand, based on previous studies of related ruthenium complexes [6,23,24]. As previously noted, chain lengthening from C≡CPh (**1**, 30 865 cm^{-1}) to 4-C≡CC_6H_4C≡CPh (**2**, 25 575 cm^{-1}) results in a red-shift in ν_{max}, as does progression from the linear compound **2** to the octopolar complex **3** (22 730 cm^{-1}). ^{1}H-NMR spectra contain phenyl and methylene resonances in the expected ratios and, for each complex, a single phosphorus signal in the ^{31}P-NMR spectrum (15.9–16.4 ppm) confirms the presence of *trans*-coordination of the diphosphine ligands at osmium; for **3**, the absence of IR bands corresponding to the C≡CH unit, or ethnyl proton resonances in the ^{1}H-NMR, confirm tri-metallation.

2.2. Electrochemical studies

Cyclic voltammetric studies were carried out on complexes **1–3** (room temperature, scan rates of ca. 100 mV s^{-1}, dichloromethane solvent) and reveal a reversible oxidation process for each complex in the range 0.36–0.39 V (Table 1) which can be assigned to the $Os^{II/III}$ couple. Previous studies on the analogous ruthenium complexes have shown no change in oxidation potential in moving from [Ru(C≡CPh)Cl(dppe)$_2$] to the chain-lengthened [Ru(C≡CC_6H_4C≡CPh)Cl(dppe)$_2$] [6], in contrast to the present series, where oxidation of the chain-lengthened osmium complex **2** is 0.03 V more difficult than the phenylacetylide complex **1**. Progression from **2** to the octopolar complex **3** results in no change in oxidation potential, as expected.

We have previously commented that phenylacetylide ligands behave (electronically) as pseudo-chlorides in ruthenium complexes of this type [22]. The same trend is seen with these osmium complexes, with the oxidation potential for *trans*-[$OsCl_2$(dppe)$_2$] (0.38 V) very similar to those of the alkynyl complexes reported herein. The synthetic precursor *cis*-[$OsCl_2$(dppe)$_2$] is, in contrast, far more difficult to oxidize (0.78 V), as expected.

In situ oxidation of **1–3** in an OTTLE cell provides a convenient method for obtaining the electronic spectra of the corresponding cationic complexes $\mathbf{1}^+$–$\mathbf{3}^+$, results being summarized in Table 1, and representative traces being shown in Figures 1 (**2**) and 2 (**3**). In contrast to the neutral complexes, which are optically transparent below 20 000 cm^{-1}, complexes $\mathbf{1}^+$–$\mathbf{3}^+$ each display a low energy band in the region 11 000–14 000 cm^{-1}, with that for **3** in particular being very intense. To understand the origin of the spectral bands in the resting and oxidized forms of **1–3**, TD-DFT calculations were carried out.

2.3. Computational studies

We have previously employed TD-DFT to calculate optical transitions in alkynylruthenium complexes [6,23], with good correlations between experimental and calculated results being obtained. As with our alkynylruthenium complex calculations, the coordinate system used in the geometry optimization for the osmium complexes was maintained for subsequent calculations of optical excitation energies. The calculated frequencies and oscillator strengths from TD-DFT studies are summarized in Table 2, together with assignment of the most important contributions to the optical transitions. The calculations indicate that there is considerable mixing of Os d-orbitals with alkynyl and/or chloro orbitals for the major transitions. The description of the orbitals involved in the assignments in Table 2 can be appreciated from the MO diagrams shown in Figs. 3 and 4. Table 2 also contains experimental and calculated frequencies and extinction coefficients/oscillator

Table 1
Summary of electrochemical and optical data for complexes **1–3**

Complex	$E_{1/2}$ [i_{pc}/i_{pa}, ΔE_p] (V) [a] $Os^{II/III}$	ν_{max} (cm^{-1}) [ε] (10^4 M^{-1} cm^{-1})	
		[M]	$[M]^+$
(**1**) *trans*-[Os(C≡CPh)Cl(dppe)$_2$]	0.36 [1, 0.08]	30 865 [2.5]	14 000 [0.9]
(**2**) *trans*-[Os(4-C≡CC_6H_4C≡CPh)Cl(dppe)$_2$]	0.39 [1, 0.07]	25 575 [2.7]	11 425 [0.4] 13 130 [1.2] 22 440 [1.1] 23 220 [1.9] 40 410 [6.5]
(**3**) 1,3,5-{*trans*-[OsCl(dppe)$_2$(4-C≡CC_6H_4C≡C)]}$_3$$C_6H_3$	0.39 [1, 0.08]	22 730 [10.2] 24 330 [1.7] 36 100 [3.0]	13 240 [5.9]

[a] In CH_2Cl_2, Ag wire reference electrode, ferrocene/ferrocenium couple at 0.56 V [1, 0.08].

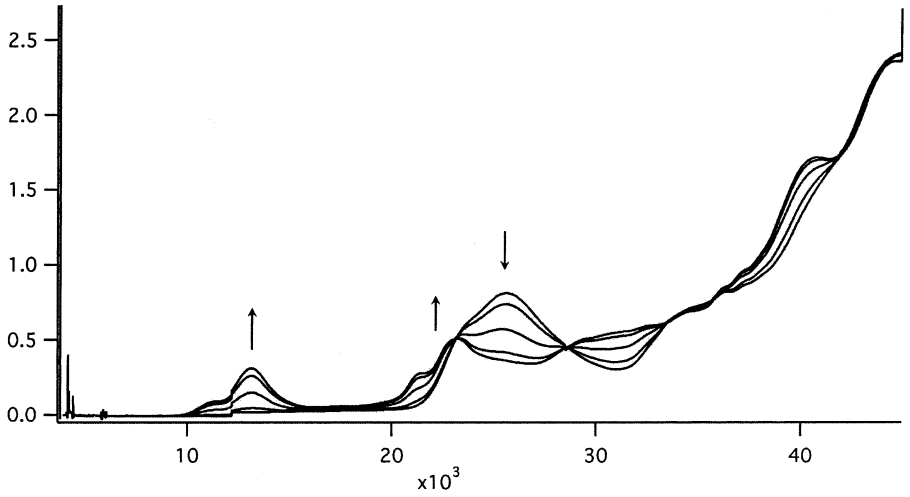

Fig. 1. UV–Vis–NIR spectral changes during electrochemical oxidation of *trans*-[Os(4-C≡CC$_6$H$_4$C≡CPh)Cl(dppe)$_2$] (**2**).

strengths. The calculated transition energies and oscillator strengths are generally in good agreement with the experimental results, differences being about 2000 cm^{-1}; these differences are most likely due to a combination of vibrational effects, gas-phase modelling and replacement of each dppe by two computationally simpler PH_3 ligands. The calculations suggest that the electronic spectra of **1** and **2** contain a metal-to-alkynyl charge-transfer band as the dominant low-energy transition. The calculations also suggest that, in both cases, metal-to-phosphorus charge-transfer plays a significant role, and that, for **2**, a low energy band is present which is not observed experimentally. These observations are broadly similar to those for the analogous ruthenium complexes [6], the notable difference being an increase in energy of the calculated and observed transitions, in most instances, upon replacing osmium with ruthenium.

The assignment of the low-lying optical transitions in the oxidized complexes has been determined by the ΔSCF method because oxidized complexes are open-shell in nature. The transition has been assumed to be owing to excitation of an electron from a low energy level into the 'hole' in the HOMO because the low-lying transitions are lower in energy than the HOMO–LUMO energy gap. Further, as all significant absorptions in the complexes **1** and **2** are due to A_1 symmetry transitions, it is probable that, for **1**$^+$ and **2**$^+$, the transition also has A_1 symmetry. Table 3 lists experimental results and calculated energy level gaps, revealing that the calculated values correlate well with the experimental results for the oxidized species. Some predicted transitions were not observed, presumably owing to poor overlap between the relevant orbitals. Figs. 3 and 4 show that the HOMO–LUMO energy

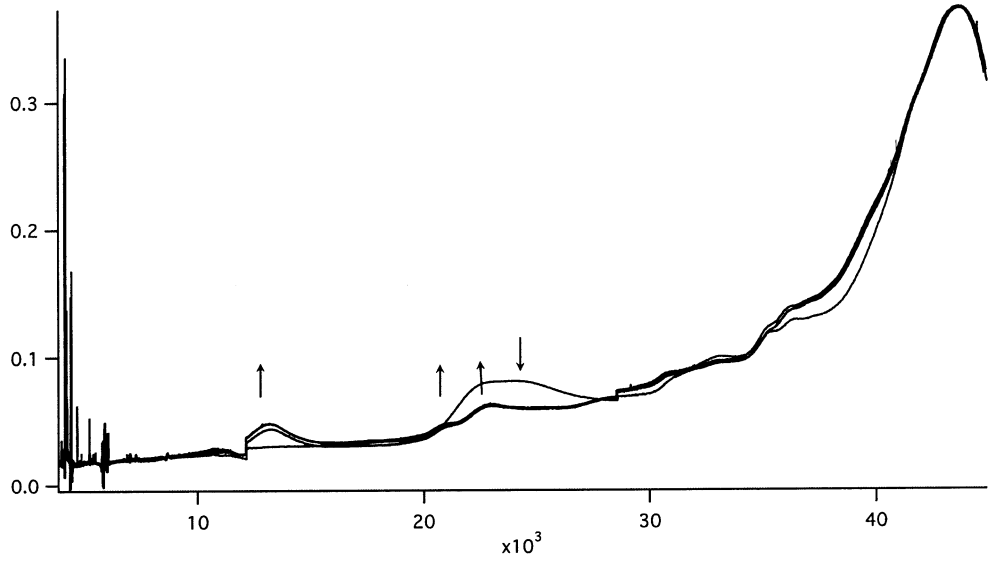

Fig. 2. UV–Vis–NIR spectral changes during electrochemical oxidation of 1,3,5-{*trans*-[OsCl(dppe)$_2$(4-C≡CC$_6$H$_4$C≡C)]}$_3$C$_6$H$_3$ (**3**).

Table 2
Calculated optical transitions for model complexes and observed values for synthesized complexes [a]

Experimental		Calculated		Symmetry	Composition	Assignment
ν_{max}	[ε]	ν_{max}	[f]			
(**1**) *trans*-[Os(C≡CPh)Cl(PH$_3$)$_4$]						
30 865	[2.5]	28 300	[0.32]	A_1	85% $10b_2 \rightarrow 11b_2$	Os $d_{yz} \rightarrow C_2Ph$
		29 600	[0.024]	A_1	96% $13b_1 \rightarrow 14b_1$	Os $d_{xz} \rightarrow PH_3$
		30 700	[0.011]	A_1	96% $10b_2 \rightarrow 12b_2$	Os $d_{yz} \rightarrow PH_3$
		31 100	[0.010]	B_1	88% $9b_2 \rightarrow 6a_2$	Os $d_{yz} \rightarrow$ Os $d_{x2-y2} + PH_3$
(**2**) *trans*-[Os(4-C≡CC$_6$H$_4$C≡CPh)Cl(PH$_3$)$_4$]						
Not observed		19 900	[0.66]	A_1	91% $13b_2 \rightarrow 14b_2$	Os $d_{yz} \rightarrow C_2R$
25 575	[2.7]	27 400	[0.39]	A_1	74% $12b_2 \rightarrow 14b_2$	Os $d_{yz} \rightarrow C_2R$
		28 500	[0.43]	A_1	77% $13b_2 \rightarrow 15b_2$	Os $d_{yz} \rightarrow C_2R$
		29 800	[0.10]	A_1	93% $13b_2 \rightarrow 16b_2$	Os $d_{yz} \rightarrow PH_3$
		31 100	[0.014]	A_1	97% $19b_1 \rightarrow 20b_1$	Os $d_{xz} \rightarrow PH_3$

[a] ν_{max} in cm^{-1}; [ε], [f] in 10^4 M^{-1} cm^{-1}.

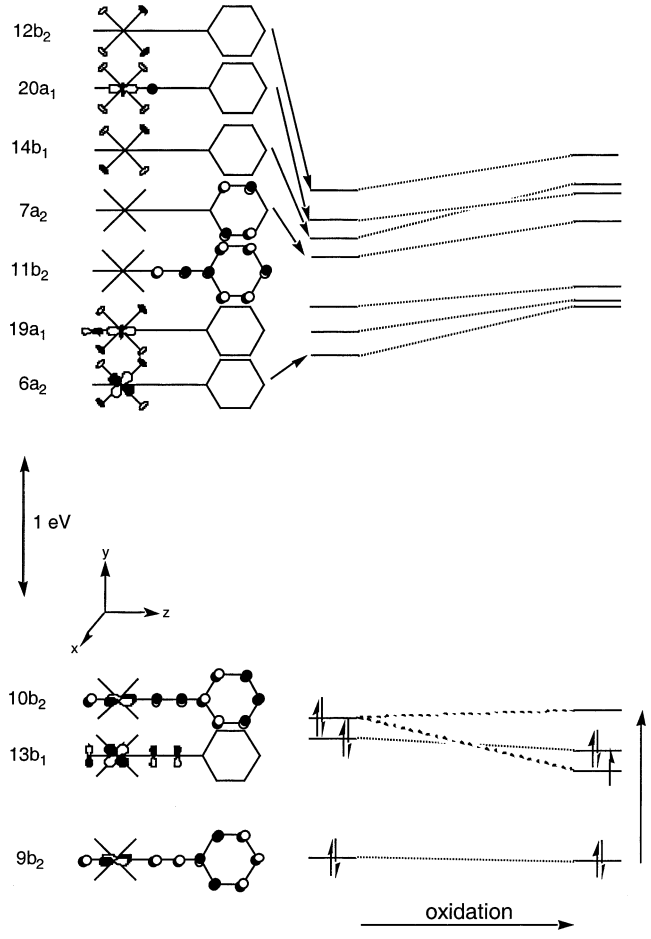

Fig. 3. Molecular orbital diagram of *trans*-[Os(C≡CPh)Cl(PH$_3$)$_4$].

difference for *trans*-[Os(C≡CPh)Cl(PH$_3$)$_4$] is considerably larger than that for *trans*-[Os(4-C≡CC$_6$H$_4$C≡CPh)Cl(PH$_3$)$_4$]. The HOMOs of both complexes are very similar in character, being delocalized about the Os d_{yz} and p_y orbitals. Whereas the LUMO of *trans*-[Os(C≡CPh)Cl(PH$_3$)$_4$] is mostly Os d_{xz} in nature, with small amounts of P s-orbital character mixed in, the LUMO of *trans*-[Os(4-C≡CC$_6$H$_4$C≡CPh)Cl(PH$_3$)$_4$] is mostly alkynyl π* character in nature. The differing LUMOs result from additional stabilization of the alkynyl π* orbital due to extra conjugation in proceeding from *trans*-[Os(C≡CPh)Cl(PH$_3$)$_4$] to *trans*-[Os(4-C≡CC$_6$H$_4$C≡CPh)Cl(PH$_3$)$_4$] (this orbital is the LUMO+2 orbital in *trans*-[Os(C≡CPh)Cl(PH$_3$)$_4$], and the LUMO in *trans*-[Os(4-C≡CC$_6$H$_4$C≡CPh)Cl(PH$_3$)$_4$]). The HOMOs and LUMOs of *trans*-[Os(C≡CPh)Cl(PH$_3$)$_4$] and *trans*-[Os(4-C≡CC$_6$H$_4$C≡CPh)Cl(PH$_3$)$_4$] are very similar to those of the ruthenium analogues. Upon oxidation of the osmium complexes, there is a small increase in the frontier orbital gap, as is apparent from Figs. 3 and 4.

The low-energy transitions in the corresponding ruthenium complexes have been utilized to demonstrate switching of the refractive and absorptive components of the cubic optical nonlinearity at 800 nm [5,6]. The intense near-infrared transitions in the oxidized forms of the osmium complexes described in the present studies could similarly be used to switch optical nonlinearity.

3. Conclusions

The studies summarized above have involved synthesis of a series of *trans*-configured alkynylchloroosmium complexes and identification of intense reversible electrochromic transitions in the near-infrared region of the optical spectrum. Comparison with the cognate ruthenium complexes reveals that these transitions appear at ca. 2000 cm^{-1} higher energy in the spectra of the osmium complexes. These electrochromic transitions were utilized in the ruthenium complexes to demonstrate switching of cubic nonlinearity, the efficacy of which is dependent on a strong optical transition at the irradiation wavelength of the laser. Access to the series of

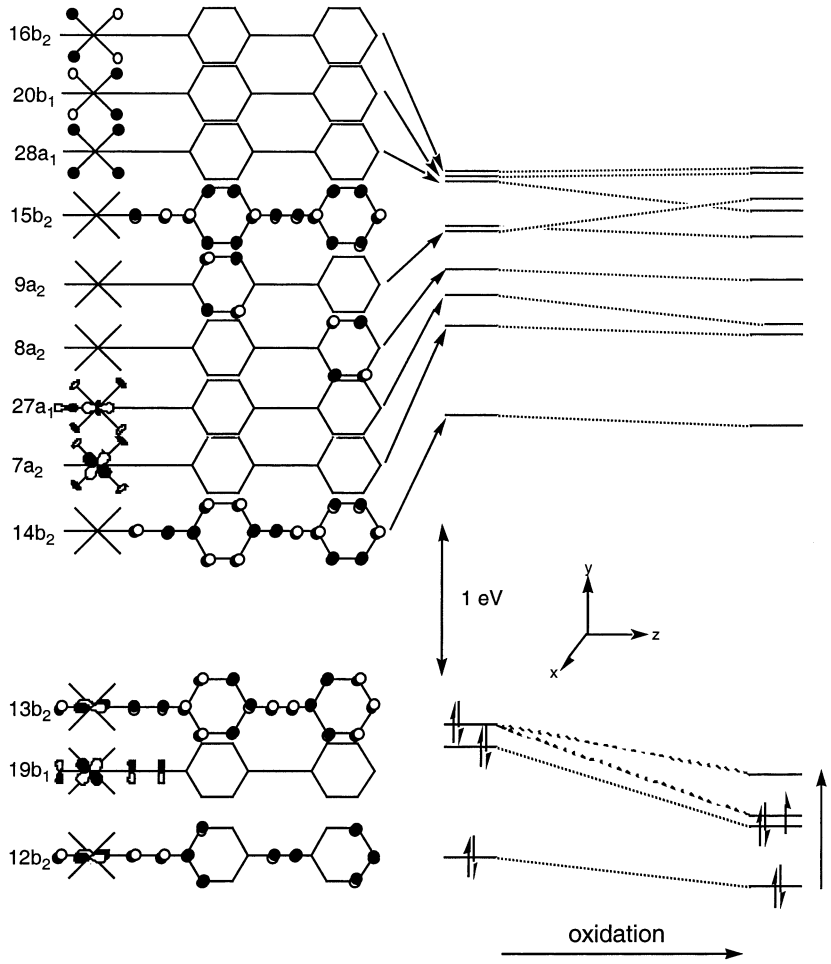

Fig. 4. Molecular orbital diagram of *trans*-[Os(4-C≡CC$_6$H$_4$C≡CPh)Cl(PH$_3$)$_4$].

osmium complexes detailed herein affords the possibility of switching nonlinearity at wavelengths complementary to that demonstrated in our earlier (ruthenium-based) report.

4. Experimental

4.1. General conditions, reagents and instruments

Reactions were performed under a nitrogen atmosphere with the use of standard Schlenk techniques with no precautions to exclude air during workup. Dichloromethane was dried by distilling over calcium hydride, diethyl ether and tetrahydrofuran were dried by distilling over sodium/benzophenone, and other solvents were used as received. "Petrol" refers to a fraction of petroleum ether of boiling range 60–80 °C. Solvents and reagents were obtained from commercial sources and used as received, unless otherwise indicated. The following were prepared according to the literature: 4-HC≡CC$_6$H$_4$C≡CPh [25], 1,3,5-C$_6$H$_3$(4-C≡CC$_6$H$_4$C≡CH)$_3$ [26], and *cis*-[OsCl$_2$(dppe)$_2$] [27].

Table 3
Observed and calculated optical transitions for **1**$^+$ and **2**$^+$ [a]

Complex	ν_{max} (experimental)	ε (experimental)	Transition	ΔE (calculated)	Assignment
1$^+$			$9b_2 \rightarrow 10b_2$	9030	Os d_{yz} + C_2Ph + Cl p_y → Os d_{yz} + C_2Ph + Cl p_y
	14 000	0.9	$8b_2 \rightarrow 10b_2$	16 620	Os d_{yz} + C_2Ph + Cl p_y → Os d_{yz} + C_2Ph + Cl p_y
			$7b_2 \rightarrow 10b_2$	22 670	C_2Ph → Os d_{yz} + C_2Ph + Cl p_y
2$^+$			$12b_2 \rightarrow 13b_2$	6210	Os d_{yz} + C_2R → Os d_{yz} + C_2R + Cl p_y
	13 130	1.2	$11b_2 \rightarrow 13b_2$	11 410	C_2Ph + Cl p_y → Os d_{yz} + C_2R + Cl p_y
	23 220	1.9	$10b_2 \rightarrow 13b_2$	17 260	Os d_{yz} + Cl p_y → Os d_{yz} + C_2R + Cl p_y

[a] ν_{max} in cm^{-1}; [ε], [f] in 10^4 M^{-1} cm^{-1}.

Atmospheric pressure chemical ionization mass spectra (APCIMS) were obtained using a Micromass/Waters LC-ZMD mass spectrometer at the Australian National University, and fast atom bombardment mass spectra (FABMS) were obtained using a VG ZAB 2SEQ instrument (30 kV Cs^+ ions, 1 mA, accelerating potential 8 kV, 3-nitrobenzyl alcohol matrix, solutions in CH_2Cl_2) at the University of Western Australia; peaks are reported as *m*/*z* (assignment, relative intensity). Microanalyses were carried out by the Microanalysis Service Unit, Australian National University. Infrared spectra were recorded as dichloromethane solutions using a Perkin–Elmer System 2000 FT-IR. ^{1}H- and ^{31}P-NMR spectra were recorded using a Varian Gemini-300 FT-NMR spectrometer and are referenced to residual chloroform (7.24 ppm) or external 85% H_3PO_4 (0.0 ppm), respectively. UV–Vis spectra were recorded as the solutions in 1 cm quartz cells using a Cary 4 spectrophotometer.

Electrochemical measurements were recorded using a MacLab 400 interface and MacLab potentiostat from ADInstruments. The supporting electrolyte was 0.1 M $(NBu^n_4)PF_6$ in distilled, deoxygenated CH_2Cl_2. Solutions containing ca. 1×10^{-3} M complex were maintained under argon. Measurements were carried out at room temperature using platinum disc working-, platinum wire auxiliary- and silver wire reference-electrodes, such that the ferrocene/ferrocenium redox couple was located at 0.56 V (peak separation ca. 0.08 V). Scan rates were typically 100 mV s^{-1}. Electronic spectra (45 000–4000 cm^{-1}) were recorded on a Cary 5 spectrophotometer. Solution spectra of the oxidized species at 253 K were obtained by electrogeneration (Thompson 401E potentiostat) at a platinum gauze-working electrode within a cryostated OTTLE cell, path length 0.5 mm, mounted within the spectrophotometer [28]. The electrogeneration potential was ca. 250 mV beyond $E_{1/2}$ for each couple, to ensure complete electrolysis. The efficiency and reversibility of each step was tested by applying a sufficiently negative potential to reduce the product; stable isosbestic points were observed in the spectral progressions for all the transformations reported herein.

DFT calculations were performed on a Linux-based Pentium IV computer (1.7 GHz) using the Amsterdam Density Functional Program (ADF) Release 1999 [29–31]. The local exchange correlation approximation of Vosko et al. [32] was used with the corrections of Becke [33] and Perdew et al. [34,35]. Type III basis sets were used for all atoms with the exception of Os, which used Type IV. Core orbitals were frozen through 1s (C), 2p (P, Cl) and 4f (Os). Relativistic corrections were incorporated using the ZORA functionality [36]. Geometries were optimized using the algorithm of Versluis and Ziegler [37]. Optical spectra were calculated using the TD-DFT functionality available in ADF [38].

4.2. Syntheses of metal complexes

4.2.1. *trans*-[Os(C≡CPh)Cl(dppe)$_2$] (**1**)

A mixture of *cis*-[$OsCl_2$(dppe)$_2$] (106 mg, 0.100 mmol), NH_4PF_6 (20 mg, 0.123 mmol) and phenylacetylene (0.5 ml, 5 mmol) was heated in refluxing toluene (10 ml) for 18 h. The solution was allowed to cool to room temperature before being filtered into rapidly stirring diethyl ether. The precipitate was collected and dissolved in the minimum amount of dichloromethane (5 ml). Triethylamine (2 ml) was added, and the mixture stirred for a further 2 h. Addition of petrol (25 ml) afforded a suspension which was collected, dissolved in the minimum amount of dichloromethane, and passed through a short basic alumina plug (5 cm), eluting with 1:1 dichloromethane:petrol. The solvent was reduced in volume in vacuo to give a pale yellow solid identified as **1** (50 mg, 44%). Anal. Calc. for $C_{60}H_{53}ClOsP_4$: C, 64.13; H, 4.75%. Found: C, 63.59; H, 5.65%. IR: ν(C≡C) 2065 cm^{-1}. UV–Vis: λ 324 nm, ε 25 000 M^{-1} cm^{-1}. ^{1}H-NMR: δ 2.53 (m, 8H, CH_2), 6.70–7.66 (m, 45H, Ph) ppm. ^{31}P-NMR: δ 16.4 ppm. APCIMS: 1051 ([OsCl(CO)(dppe)$_2$]$^+$, 100), 1016 ([Os(CO)(dppe)$_2$]$^+$, 7), 988 ([Os(dppe)$_2$]$^+$, 3).

4.2.2. *trans*-[Os(4-C≡CC_6H_4C≡CPh)Cl(dppe)$_2$] (**2**)

A mixture of *cis*-[$OsCl_2$(dppe)$_2$] (100 mg, 0.10 mmol), NH_4PF_6 (20 mg, 0.12 mmol) and 4-HC≡CC_6H_4C≡CPh (23 mg, 0.11 mmol) was heated in refluxing toluene (10 ml) for 18 h. The solution was allowed to cool to room temperature and filtered into rapidly stirring diethyl ether. The precipitate was collected and dissolved in the minimum amount of dichloromethane (5 ml). Triethylamine (2 ml) was added and the mixture stirred for a further 2 h. Addition of petrol (25 ml) afforded a suspension which was collected, dissolved in the minimum amount of dichloromethane, and passed through a short basic alumina plug (5 cm), eluting with 1:1 dichloromethane:petrol. The solvent was reduced in volume in vacuo to give a yellow solid identified as **2** (45 mg, 36%). Anal. Calc. for $C_{68}H_{57}ClOsP_4$: C, 66.74; H, 4.69%. Found: C, 68.22; H, 5.34%. IR: ν(C≡C) 2057 cm^{-1}. UV–Vis: λ 391 nm, ε 26 600 M^{-1} cm^{-1}. ^{1}H-NMR: δ 2.60 (m, 8H, CH_2), 6.57–7.50 (m, 49H, C_6H_4+Ph) ppm. ^{31}P-NMR: δ 15.9 ppm. SIMS: 1224 ([M]$^+$, 100), 1189 ([M−Cl]$^+$, 6), 1123 ([M−C≡CPh]$^+$, 5), 1051 ([OsCl(CO)(dppe)$_2$]$^+$, 3), 988 ([Os(dppe)$_2$]$^+$, 6).

4.2.3. 1,3,5-{*trans*-[OsCl(dppe)$_2$(4-C≡CC_6H_4C≡C)]}$_3C_6H_3$ (**3**)

A mixture of *cis*-[$OsCl_2$(dppe)$_2$] (150 mg, 0.15 mmol), NH_4PF_6 (23 mg, 0.13 mmol) and 1,3,5-C_6H_3(4-C≡CC_6H_4C≡CH)$_3$ (21 mg, 0.045 mmol) was heated in refluxing toluene (15 ml) for 18 h. The solution was allowed to cool to room temperature and filtered into rapidly stirring diethyl ether. The resultant solid was

collected and dissolved in the minimum amount of dichloromethane (5 ml). Triethylamine (2 ml) was added and the mixture stirred for a further 2 h. Addition of petrol (25 ml) afforded a suspension which was collected, dissolved in the minimum amount of dichloromethane, and passed through a short basic alumina plug (5 cm), eluting with 1:1 dichloromethane:petrol. The solvent was reduced in volume in vacuo to give a pale yellow solid identified as **3** (54 mg, 37%). Satisfactory microanalyses could not be obtained owing to slow sample decomposition. IR: ν(C≡C) 2061 cm^{-1}. UV–Vis: λ 277 nm, ε 30 200 M^{-1} cm^{-1}; 411 nm, ε 17 300 M^{-1} cm^{-1}; 440 nm, ε 17 700 M^{-1} cm^{-1}. ^{1}H-NMR: δ 2.60 (m, 24H, CH_2), 6.57–7.50 (m, 135H, C_6H_4+Ph) ppm. ^{31}P-NMR: δ 15.9 ppm. SIMS: 1246 ($[Os(C_2C_6H_4C_2C_6H_3C_2)Cl(dppe)_2]^+$, 25), 1123 ($[Os(C_2C_6H_4)Cl(dppe)_2]^+$, 10), 1051 ($[OsCl(CO)(dppe)_2]^+$, 100), 1023 ($[OsCl(dppe)_2]^+$, 15), 1016 ($[Os(CO)(dppe)_2]^+$, 17), 988 ($[Os(dppe)_2]^+$, 25).

Acknowledgements

We thank the Australian Research Council (M.G.H. and M.P.C) for support of this work, and Johnson-Matthey Technology Centre (M.G.H) for the generous loan of osmium. M.P.C. holds an ARC Australian Research Fellowship and M.G.H. holds an ARC Australian Senior Research Fellowship.

References

[1] S.K. Hurst, M.G. Humphrey, J.P. Morrall, M.P. Cifuentes, M. Samoc, B. Luther-Davies, G.A. Heath, A.C. Willis, J. Organomet. Chem., in press.
[2] T. Verbiest, S. Houbrechts, M. Kauranen, K. Clays, A. Persoons, J. Mater. Chem. 7 (1997) 2175.
[3] I.R. Whittall, A.M. McDonagh, M.G. Humphrey, M. Samoc, Adv. Organomet. Chem. 42 (1998) 291.
[4] I.R. Whittall, A.M. McDonagh, M.G. Humphrey, M. Samoc, Adv. Organomet. Chem. 43 (1999) 349.
[5] M.P. Cifuentes, C.E. Powell, M.G. Humphrey, G.A. Heath, M. Samoc, B. Luther-Davies, J. Phys. Chem. A. 105 (2001) 9625.
[6] C.E. Powell, M.P. Cifuentes, J.P.L. Morrall, R. Stranger, M.G. Humphrey, M. Samoc, B. Luther-Davies, G.A. Heath, J. Am. Chem. Soc., 125 (2003) 602.
[7] B.J. Coe, S. Houbrechts, I. Asselberghs, A. Persoons, Angew. Chem. Int. Ed. Engl. 38 (1999) 366.
[8] R. Denis, L. Toupet, F. Paul, C. Lapinte, Organometallics 19 (2000) 4240.
[9] M. Malaun, Z.R. Reeves, R.L. Paul, J.C. Jeffery, J.A. McCleverty, M.D. Ward, I. Asselberghs, K. Clays, A. Persoons, Chem. Commun. (2001) 49.
[10] C.D. Delfs, R. Stranger, M.G. Humphrey, A.M. McDonagh, J. Organomet. Chem. 607 (2000) 208.
[11] N.J. Long, A.J. Martin, A.J.P. White, D.J. Williams, M. Fontani, F. Lashi, P. Zanello, J. Chem. Soc. Dalton Trans. (2000) 3387.
[12] M. Younus, N.J. Long, P.R. Raithby, J. Lewis, N.A. Page, A.J.P. White, D.J. Williams, M.C.B. Colbert, A.J. Hodge, M.S. Khan, D.G. Parker, J. Organomet. Chem. 578 (1999) 198.
[13] M. Younus, N.J. Long, P.R. Raithby, J. Lewis, J. Organomet. Chem. 570 (1998) 55.
[14] M.C.B. Colbert, J. Lewis, N.J. Long, P.R. Raithby, M. Younus, A.J.P. White, D.J. Williams, N.N. Payne, L. Yellowlees, D. Beljonne, N. Chawdhury, R.H. Friend, Organometallics 17 (1998) 3034.
[15] J. Lewis, P.R. Raithby, W.-Y. Wong, J. Organomet. Chem. 556 (1998) 219.
[16] N.J. Long, A.J. Martin, F. Fabrizi de Biani, P. Zanello, J. Chem. Soc. Dalton Trans. (1998) 2017.
[17] M.C.B. Colbert, J. Lewis, N.J. Long, P.R. Raithby, D.A. Bloor, G.H. Cross, J. Organomet. Chem. 531 (1997) 183.
[18] A.J. Hodge, S.L. Ingham, A.K. Kakkar, M.S. Khan, J. Lewis, N.J. Long, D.G. Parker, P.R. Raithby, J. Organomet. Chem. 488 (1995) 205.
[19] Z. Atherton, C.W. Faulkner, S.L. Ingham, A.K. Kakkar, M.S. Khan, J. Lewis, N.J. Long, P.R. Raithby, J. Organomet. Chem. 462 (1993) 265.
[20] A.M. McDonagh, M.P. Cifuentes, M.G. Humphrey, S. Houbrechts, J. Maes, A. Persoons, M. Samoc, B. Luther-Davies, J. Organomet. Chem. 610 (2000) 71.
[21] D. Touchard, P. Haquette, N. Pirio, L. Toupet, P.H. Dixneuf, Organometallics 12 (1993) 3132.
[22] A.M. McDonagh, M.G. Humphrey, M. Samoc, B. Luther-Davies, S. Houbrechts, T. Wada, H. Sasabe, A. Persoons, J. Am. Chem. Soc. 121 (1999) 1405.
[23] C.E. Powell, M.P. Cifuentes, A.M. McDonagh, S.K. Hurst, N.T. Lucas, C.D. Delfs, R. Stranger, M.G. Humphrey, S. Houbrechts, I. Asselberghs, A. Persoons, D.C.R. Hockless, J. Organomet. Chem., in press.
[24] R.H. Naulty, A.M. McDonagh, I.R. Whittall, M.P. Cifuentes, M.G. Humphrey, S. Houbrechts, J. Maes, A. Persoons, G.A. Heath, D.C.R. Hockless, J. Organomet. Chem. 563 (1998) 137.
[25] O. Lavastre, S. Cabioch, P.H. Dixneuf, J. Vohlidal, Tetrahedron 53 (1997) 7595.
[26] A.M. McDonagh, C.E. Powell, J.P.L. Morrall, M.P. Cifuentes, M.G. Humphrey, Organometallics, in press.
[27] P.G. Antonov, Y.N. Kukushkin, V.I. Konnov, Y.P. Kostikov, Koord. Khim. 6 (1980) 1585.
[28] C.M. Duff, G.A. Heath, Inorg. Chem. 30 (1991) 2528.
[29] E.J. Baerends, P. Ros, Chem. Phys. 2 (1973) 42.
[30] E.J. Baerends, P. Ros, Chem. Phys. 2 (1973) 52.
[31] E.J. Baerends, P. Ros, Int. J. Quant. Chem. S12 (1978) 169.
[32] S.H. Vosko, L. Wilk, M. Nusair, Can. J. Phys. 58 (1980) 1200.
[33] A.D.J. Becke, Chem. Phys. 84 (1986) 4524.
[34] J.P. Perdew, Phys. Rev. B 33 (1986) 8822.
[35] J.P. Perdew, J.A. Chevary, S.H. Vosko, K.A. Jackson, M.R. Pederson, D.J. Singh, C. Fiolhais, Phys. Rev. A 46 (1992) 6671.
[36] E. van Lenthe, E.J. Baerends, J.G.J. Snijders, Chem. Phys. 99 (1993) 4597.
[37] L. Versluis, T. Ziegler, J. Chem. Phys. 88 (1988) 322.
[38] S.J.A. van Gisbergen, J.G. Snijders, E.J. Baerends, Comput. Phys. Commun. 118 (1999) 119.